Slipping Behavior and Relaxation Characteristics of Thin-Walled GFRP High-Strength Bolted Friction Joints for Sound Barriers on Bridge Viaducts

Slipping behavior and relaxation characteristics of thin-walled GFRP high-strength bolted friction joints for sound barriers on bridge viaducts

Masaki Sekimoto, Gen Hayashi, Takashi Yamaguchi

Osaka Metropolitan University, Osaka, Japan

Keiichi Sakai, Kai Aoki, Keigo Kubo

Miyaji Engineering Co. Ltd., Tokyo, Japan

Contact: sekimoto@brdg.civil.eng.osaka-cu.ac.jp, hayashi-g@omu.ac.jp

Abstract

This study aimed to clarify the performance of high-strength bolted joints for thin-walled glass-fiber-reinforced polymer (GFRP) members by conducting slip tests and long-term relaxation tests. The parameters of the slip test were the FRP surface treatment, bolt axial force, and bolt hole diameter. Relaxation characteristics might also be affected by variations in fiber content based on differences in production lots. Hence, samples from different production lots were taken. However, in these tests, the influence of all parameters was relatively minimal. One year after tightening, the axial force reduction gradually subsided and tended toward convergence. However, because it is difficult to determine convergence based on temperature changes, long-term measurements will continue. In the slip tests, the highest slip coefficient was obtained when the GFRP was coated with fluoroplastic and the connecting plates were treated with phosphate. This study proposes a design slip coefficient for GFRP high-strength bolted friction joints.

Keywords: GFRP, high-strength bolted friction joints, slipping behavior, relaxation

1 Introduction

Glass-fiber-reinforced polymer (GFRP) has excellent material properties such as corrosion resistance, high strength and light weight. Moreover, laminated structures made from GFRP can be easily molded to form single parts. This reduces cost and simplifies manufacturing processes [1]. This has the advantage of simplifying the structure of bridge appendages such as GFRP wall railings, which are complex structures with many components. Therefore, the number of components can be reduced and workability improved, which has led to its application to bridge appendages. High-strength bolted friction joints, which have a proven track record in steel structures and are highly reliable, are commonly used.

However, in GFRP members with these joints, creep deformation occurs after a certain period of time owing to the viscoelastic behavior of the matrix resin after axial force is introduced. Therefore, the bolt axial force may be reduced to a greater extent than that in general steel.

Mottram et al. [2] demonstrated that the axial force reduces by approximately 25% within 18 days after bolting for FRP joints consisting solely of pultruded FRP. They also calculated that the axial force would decrease by approximately 36% in the first year after tightening.

However, data were only available for 18 days. Long-term measurements are required. Few studies have been conducted on the relaxation properties of thin-walled GFRP members, which are the subject of this research. Furthermore, there has been little research on the structural parameters affecting the sliding behavior of GFRP joints; moreover, design criteria for high-strength bolted friction joints have not been developed.

In this study, long-term relaxation tests and tensile tests were conducted on the thin GFRP joints used in wall-high column joints to investigate the performance of GFRP joints considering joint surface treatment as a parameter.

2 Long-term Relaxation Tests

2.1 Specimens and parameters

Figure 1 presents the geometric dimensions of the test specimens. The base plate is a GFRP pultrusion-molded material, the connecting plates are hot-dip galvanized SS400, and the bolts are M20 (F8T) hot-dip galvanized high-strength bolts. There are five bolts per specimen. The distance between bolts is unaffected by the surface pressure of the adjacent bolts.

The GFRP laminate configuration consists of six layers of roving, unidirectional roving cloth, and continuous strand mats starting from the center of the plate thickness with the outermost surface of the member being a non-woven polyester. The resin material is unsaturated polyester resin.

Table 1 lists the specimen parameters. The parameter for the joint surface treatment is the presence or absence of a fluoropolymer coating for the GFRP. The diameters of the holes are defined according to an enlarged hole (ϕ24.5) and standard hole (ϕ22). The introduced bolt axial force is 100% of the axial force and is applied using the nut rotation method. Additionally, according to Ref. [3], the results of a one-year long-term relaxation test

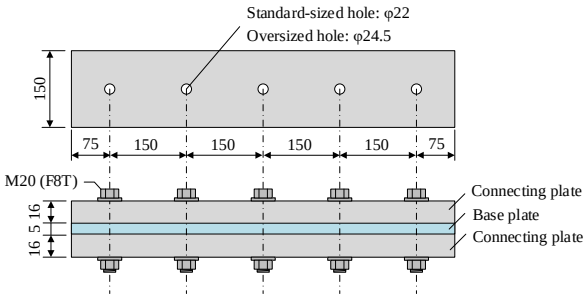

Figure 1. Specimen dimensions (unit: mm)

Table 1. Parameter for the long-term relaxation test case

Case	Surf. coating of GFRP	Bolt hole	Axial force	Production lot
U-O-80-R1	Unpainted	Over(φ24.5)	80%	No.1
U-O-100-R1	Unpainted	Over(φ24.5)	100%	No.1
P-O-100-R1	Painted	Over(φ24.5)	100%	No.1
U-S-100-R1	Unpainted	Standard(φ22)	100%	No.1
U-O-100-R2	Unpainted	Over(φ24.5)	100%	No.2

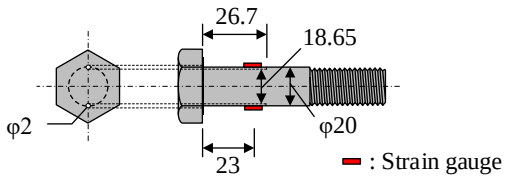

Figure 2. Strain gauged bolt (unit: mm)

on a specimen with GFRP as a base plate and steel plates as connecting plates revealed that the axial force was reduced by approximately 20%. Therefore, a case with an introduced bolt axial force of 80% was also conducted to account for this reduction in axial force. Furthermore, the variation in fiber content based on differences in production lots was also considered. The combustion test results that measured the mass of the specimens before and after burning indicated that the fiber contents of Lots 1 and 2 were 58% and 54%, respectively.

2.2 Long-term relaxation test methods

The tightening procedure for the U-O-100-R1 specimen was as follows. (1) A gauge bolt was placed on the specimen. (2) As a preliminary

Table 2. Tightening results and axial force residual ratios

Case	Bolt No.	Angle of rotation	Initial axial force(kN)		Residual axial force(%) After 1 day			Residual axial force(%) After 1 year		
				mean		mean	C.V.(%)		mean	C.V.(%)
U-O-80-R1	1	60	156.6	155.5	89.8	92.2	2.72	83.6	85.9	2.88
	2	70	156.2		90.3			83.6		
	3	60	155.4		91.1			85.1		
	4	85	152.2		96.7			90.3		
	5	115	157.1		93.2			86.7		
U-O-100-R1	6	120	192.6	194.1	92.8	91.5	0.78	86.7	85.7	0.66
	7	120	200.5		91.1			85.5		
	8	120	196.4		91.2			85.5		
	9	120	193.1		90.8			85.0		
	10	120	188.1		91.5			85.6		
P-O-100-R1	16	120	194.4	192.2	91.6	91.4	1.59	85.5	85.3	1.60
	17	120	189.1		93.7			87.4		
	18	120	192.3		90.5			84.6		
	19	145	187.2		86.5			80.6		
	20	120	192.9		90.0			83.7		
U-S-100-R1	21	70	191.2	191.2	90.9	90.9	0.28	85.0	85.1	0.37
	22	120	175.8		95.6			89.2		
	23	115	190.6		90.6			84.8		
	24	90	163.8		95.4			89.2		
	25	120	191.6		91.3			85.5		
U-O-100-R2	26	130	192.9	192.3	91.5	91.0	0.38	85.3	84.6	0.55
	27	130	191.8		91.0			84.4		
	28	120	193.0		90.7			84.6		
	29	135	191.6		90.6			84.0		
	30	150	176.1		84.6			78.9		

tightening step, the bolts were tightened to the order of 150 Nm of torque from the inside bolt to the outside bolt of the specimen. (3) Marking bolts, nuts, washers, and members were installed. (4) The nut rotation method was used for primary tightening, where tightening was performed from pre-tightening to a rotation angle of 120°. The nut rotation method introduces an axial force that is 1.4 to 1.5 times the designed bolt axial force.

In the other cases, the axial force of U-O-100-R1 was set to 100% and clamping was performed using strain control.

The initially introduced bolt axial force was measured 3 s after the peak of tightening [4] and the axial force was measured at 1 s intervals until 1 h after tightening, at 1 min intervals until 24 h after tightening, and at 15 min intervals thereafter. One specimen was tested in each case.

2.3 Test results and discussions

Table 2 presents the tightening results for all specimens and the percentages of axial force remaining after one day and one year of tightening. The specimens highlighted in red in Table 2 could not provide sufficient axial force for co-rotation of bolt set. Therefore, these test results were only used for reference.

Table 2 reveals that there are large variations in the rotation angle at the point of axial force introduction for the bolts tightened using strain control.

This may be a result of variations in the introduced axial force in the nut rotation method and poor engagement caused by the plating of the bolt and nut threads.

Figure 3 presents the changes in bolt axial force at one day and one year after tightening. This figure presents the values for one bolt in each case.

The decrease in bolt axial force during the first 24 h after tightening is significant. Thereafter, the axial force of the bolt slowly decreases. One year after tightening, the axial force reduction gradually subsides and trends toward convergence. However, because it is difficult to determine convergence as

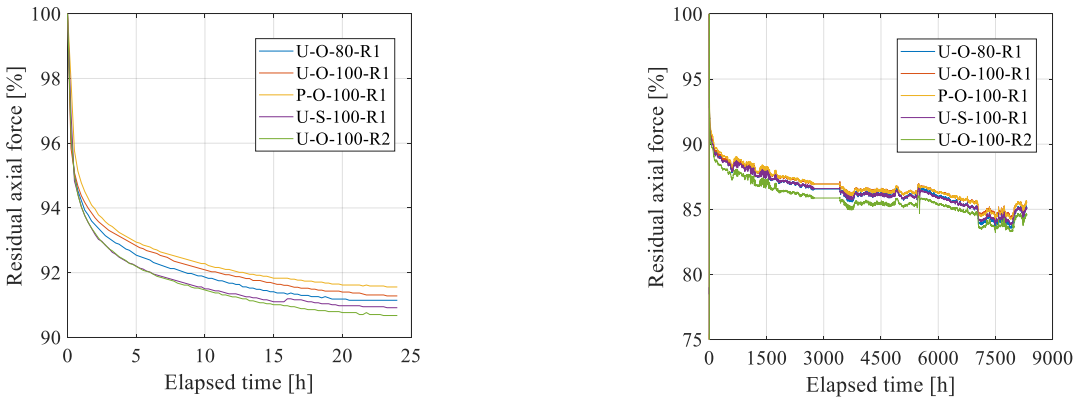

(a) One day (b) One year

Figure 3. Changes over time in bolt axial force

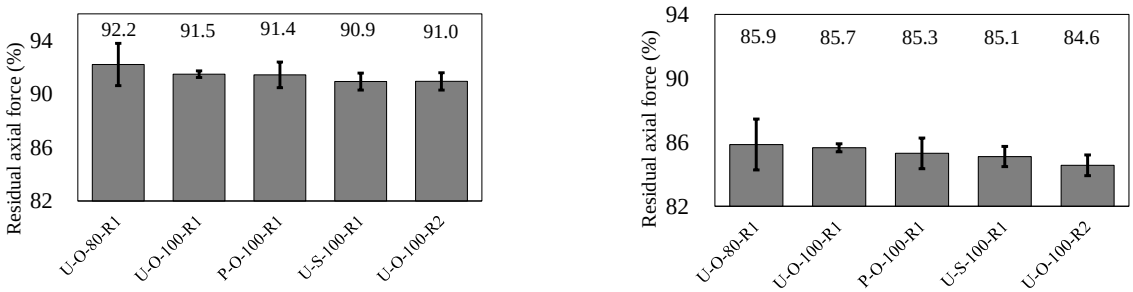

(a) One day (b) One year

Figure 4. Bolt axial force reduction rate(mean)

a result of temperature changes, long-term measurements will need to be continued.

Figure 4 presents the percentage of remaining axial force after 24 h and after one year following tightening. This figure presents the average values for each case.

In each case, the remaining axial force 24 h after tightening is approximately 91% to 92% and after one year of tightening, the remaining axial force is approximately 85%. It was determined that test parameters such as the coating on the GFRP surface, introduced bolt axial force, variations in fabrication lots, and differences between enlarged and standard holes had no effect on the test results.

In the future, it will be necessary to study the effects of differences in the fiber content, fiber composition, and molding method of GFRP specimens on axial force reduction.

3 Tensile Tests

3.1 Specimens and parameters

Figure 5 presents the geometric dimensions of the test specimens. The base plate is a GFRP pultrusion-molded material, the connecting plates are hot-dip galvanized SM400A, and M12 (F10T) bolts are used. The specimen was designed to provide surface pressure equivalent to that acting on the surface of the test specimen base plate, as shown in Figure 1, which is a full-scale equivalent. The magnitude of the surface pressure was 39.3 N/mm^2.

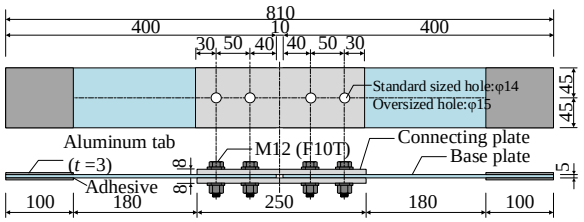

Figure 5. Specimen dimensions (unit: mm)

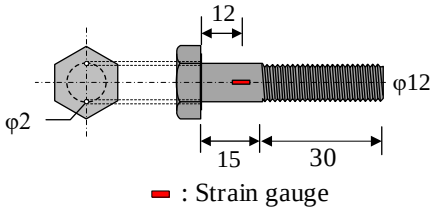

Figure 6. Strain gauged bolt (unit: mm)

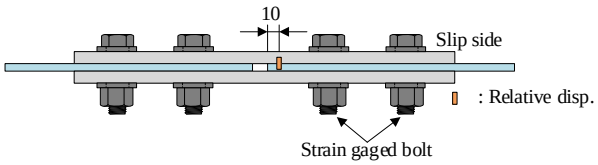

Figure 7. Measurement items and locations (unit: mm)

Table 3. Parameters for the tensile test

Case	Axial force	Surf.coating of connecting plate	Surf.coating of GFRP	Bolt hole	β
R1-80-PNL	80%	Phosphate treat.	Unpainted	Over(φ15)	0.49
R1-100-PNL	100%	Phosphate treat.	Unpainted	Over(φ15)	0.62
R1-80-PPL	80%	Phosphate treat.	Painted	Over(φ15)	0.49
R1-100-PPL	100%	Phosphate treat.	Painted	Over(φ15)	0.62
R1-100-PNN	100%	Phosphate treat.	Unpainted	Standard(φ14)	0.61
R1-100-NPL	100%	N.A.	Painted	Over(φ15)	0.62

* β: Designed slip to yield resistance ratio

Since GFRP is an elastic material with no yield point, the tensile strength in the pulling direction was used instead of the yield strength in the case of steel.

Table 4. Results for surface roughness (Ra)

Case	Surface roughness Ra(μm)	
	Base plate	Connecting plate
R1-80-PNL	1.77	10.30
R1-100-PNL	1.45	10.22
R1-80-PPL	1.14	11.09
R1-100-PPL	1.09	9.12
R1-100-PNN	1.70	11.35
R1-100-NPL	1.04	7.41

The GFRP laminate composition and resin material were the same as those used for the specimens in the long-term relaxation tests. All specimens were produced in the same lot and the fiber content was 54% to 58% based on the results of combustion tests.

Table 3 lists the specimen parameters. Based on the results of the long-term relaxation tests, the axial force of the introduced bolts was set to 100% of the axial force at four months after tightening. A case study with an introduced axial force of 80% was also conducted to reduce the axial force further. The parameters for the joint surface treatment were the presence or absence of phosphate treatment for the connecting plates and presence or absence of fluoropolymer coating for the GFRP. The diameters of the holes were defined for enlarged (ϕ15) and standard (ϕ14) holes. Five specimens were tested in each case.

Table 4 presents the surface roughness measurements for the base and connecting plates. Measurements were performed at 16 points per specimen around the bolt holes for all specimens. The thickness of the GFRP-coated surface was approximately 40 μm.

Figure 6 presents a strain gauged bolt. The bolt axial force during testing was controlled by the strain value of the strain-gauge bolt.

Tightening was performed under torque control to achieve 60% of the introduced bolt axial force for preliminary tightening. Then, as the primary tightening step, the bolts were tightened with strain control to achieve the desired bolt axial force.

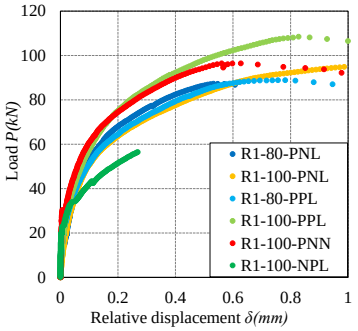

(a) Raw data

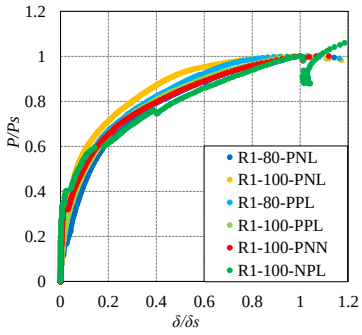

(b) Non-dimensionalized results

Figure 8. Load relative displacement relationships

3.2 Tensile testing methods

Loading was performed using a universal testing machine (maximum capacity: 2000 kN) with a loading rate of 0.5 kN/s. The specimens were unloaded before the onset of slip and transition to a bearing condition and loaded until the end state was reached.

Figure 7 presents the measurement items and their locations. The measurement items are relative displacement, testing machine load, and bolt shank strain, which were measured at the positions indicated in Figure 7. Relative displacement is the relative displacement between the baseplate and connecting plate. Bolt shank strain was measured to determine the bolt tension.

Slip coefficient was calculated using Equation (1).

$$\mu = \frac{P_s}{m \cdot n \cdot N} \qquad (1)$$

Here, P_s is the slip load, m (=2) is the number of frictional surfaces, n (=2) is the number of bolts, and N is the axial force of the bolts. The slip coefficients μ_0, μ_1, and μ_2 were calculated based on the designed bolt axial force, bolt axial force before testing, and bolt axial force during slip, respectively.

Table 5. Slip coefficient μ_0, μ_1, μ_2 (mean)

Case	Slipping load (kN)	Slip coefficient μ_0		Slip coefficient μ_1		Slip coefficient μ_2	
		mean	CV(%)	mean	CV(%)	mean	CV(%)
R1-80-PNL	80.8	0.387	5.19	0.483	4.17	0.509	8.20
R1-100-PNL	95.8	0.462	1.16	0.455	1.77	0.486	1.85
R1-80-PPL	89.4	0.429	5.13	0.540	3.40	0.573	2.39
R1-100-PPL	108.9	0.522	1.73	0.522	3.16	0.541	3.23
R1-100-PNN	96.3	0.461	2.28	0.454	1.57	0.488	1.45
R1-100-NPL	52.8	0.253	13.59	0.253	12.14	0.259	12.60

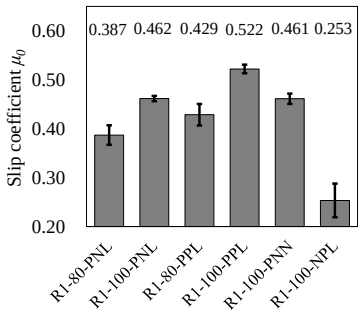

(a) μ_0

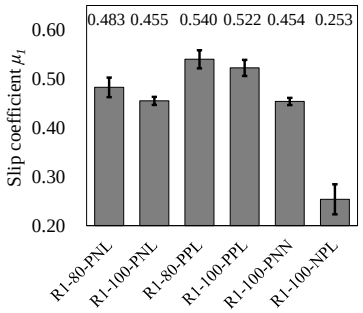

(b) μ_1

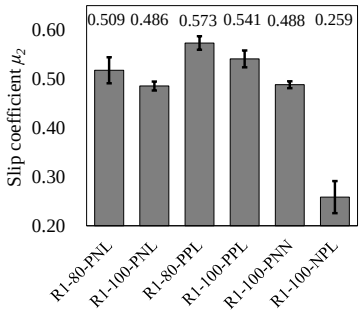

(c) μ_2

Figure 9. Slip coefficient μ_0, μ_1, μ_2 (mean)

The designed slip capacity of the specimen was 83.5 kN for the 100% axial force case and 66.8 kN for the 80% case. The shear capacity of the bolts was 291.2 kN, net section rupture capacity was 140.8 kN, and edge rupture capacity of the base plate was 39.6 kN.

3.3 Test results and discussion

Figure 8 presents the load relative displacement relationship along the 10 mm edge of the base plate. Figure 8 (a) shows the raw data and Figure 8 (b) shows the non-dimensionalized results for the load at slip and relative displacement at slip.

The relative displacement of the GFRP joints is greater than that of steel joints based on the lower stiffness of the base material. Therefore, in this test, the load on the testing machine at the time of load drop was considered as the slip load. From Figure 8 (b), it can be seen that the load relative displacement relationship is consistent, regardless of whether the specimens are phosphatized or coated with GFRP.

Table 5 and Figure 9 present the slip coefficients. It is apparent that μ_1 and μ_2 exhibit similar trends, although their values are different.

Focusing on the installed bolt axial force, the slip coefficient μ_1 at 80% is approximately 6.1% higher than that at 100% without paint and 3.4% higher than that at 100% with paint. This result is similar to a previous finding [5] that the smaller the pre-test bolt axial force, the greater is the slip coefficient.

Focusing on the coating, the slip coefficient μ_1 with the coating is approximately 11.8% higher at 80% axial force and approximately 14.7% higher at 100% axial force. This is assumed to be caused by the softness of the fluoropolymer coating and increased adhesion between the connecting plate and fluoropolymer surface after tightening.

The slip coefficient μ_1 of the connecting plate surfaces was greater than 0.40 in all cases where the plates were treated with phosphate.

However, no difference in the slip coefficients was observed between the enlarged and standard boreholes.

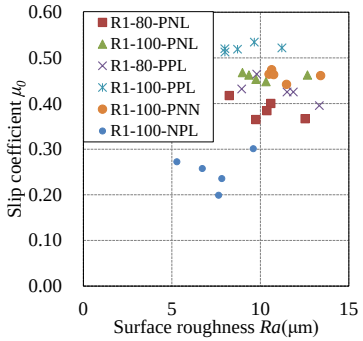

Figure 10. Relationship between the surface roughness of the connecting plate and slip coefficient μ_0

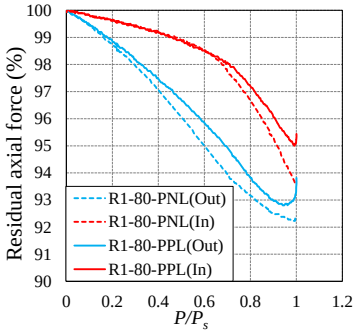

(a) Introduced axial force of 80%

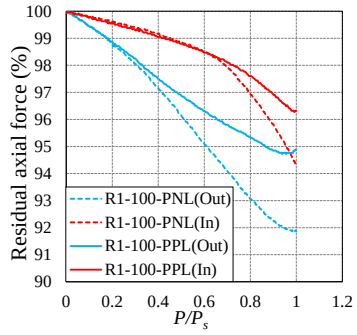

(b) Introduced axial force of 100%

Figure 11. Load axial force residual ratio relationship

Figure 10 presents the relationship between the surface roughness of the connecting plate and slip coefficient μ_0.

It can be seen that the phosphate treatment increases the surface roughness, which is thought to improve the slip coefficient. When the connecting plates are treated with phosphate, the slip coefficient μ_0 is expected to be greater than

0.40 and when GFRP is coated, the slip coefficient is increased further.

Figure 11 presents the load axial force residual ratio relationship. The abscissa is the load non-dimensionalized by the slip load and the ordinate is the percentage of remaining axial force when the pre-test bolt axial force is set to 100%.

The axial force of the outer bolt decreases at a constant rate, whereas the rate of axial force decreases for the inner bolt increases at $P / P_s = 0.6$. The axial force reduction of the GFRP with the coating was 2% to 3% smaller than that without the coating. These factors will be examined analytically in the future.

It can be seen that the difference in the amount of axial force reduction with and without coating is smaller with an introduced axial force of 80% than with an introduced axial force of 100%.

An increase in axial force was observed at the outer bolts near the slip load. This is considered to be a result of the fact that the bolts came into contact with the specimen and were subjected to bearing pressure as a result of the gradual onset of slip.

4 Conclusions

In this study, long-term relaxation tests were conducted on GFRP joints for thin plates. The results demonstrated that the remaining axial force approximately one year after tightening was almost 85% and that the coating on the GFRP surface, introduced bolt axial force, differences in production lots, size of the bolt hole had no effect on it.

Tensile tests were also conducted. It was determined that the slip coefficient μ_0 calculated from the designed bolt axial force was more than 0.40 when the surface of the GFRP was coated with fluoroplastic and the connecting plates were treated with phosphate. The slip coefficient μ_1 calculated from the bolt axial force before testing was approximately 3% to 6% at 80% of the introduced bolt axial force, approximately 11% to 14% for the GFRP with a coating, and even higher for the phosphate-treated connecting plate surfaces. However, size of bolt hole had no effect.

In long-term relaxation tests, it will be necessary to examine the effects of differences in fiber content, fiber composition, forming method, etc. on the reduction in axial force to determine the introduced bolt axial force on site. In tensile tests, a proposal for the joint surface treatment and design slip coefficient for GFRP high-strength bolted friction joints is presented.

Acknowledgments

This research was partially supported by JSPS Grants-in-Aid for Scientific Research (Issue No. 21K14234). We wish to express our gratitude for this support.

References

[1] Bibekananda Mandal, Anupam Chakrabarti: Numerical failure assessment of multi-bolt FRP composite joints with varying sizes and preloads of bolts, Composite Structures 187, pp.169-178, 2018

[2] J. T. Mottram: Friction and load transfer in bolted joints of pultruded fibre reinforced polymer section, Taylor & Francis Group plc, London, UK, 2005

[3] Takeshi Kijima, Toshio Katsuno, Kenji Kobayashi, Shin-i-chi Hino, Itaru Nishizaki: Relaxation behavior of clamping force in bolted joints of pultruded GFRP laminates, Journal of Society of Materials Science, Japan, Vol.59, No.7, pp540-545, 2010 (in Japanese)

[4] Kuniaki Minami, Hiroshi Tamura, Daisuke Uchida, Hiromi Shirahara, Natsuki Yoshioka, Kouhei Tsutsuji, Daichi Fujino: A study on initial value setting method for relaxation tests in high strength bolted joints, Journal of JSCE, Vol.76, No.3, pp.496-509, 2020 (in Japanese)

[5] Takeshi Mori, Takeo Amitani, Daisuke Uchida: Influence of bolt tightening force on slip coefficient of high-strength bolted friction type joints, Journal of JSCE, No.1, pp.58-66, 2019 (in Japanese)